

Control of mean diameter and size distribution during formulation of microcapsules with cellulose nitrate membranes

B. Poncelet De Smet, D. Poncelet and R. J. Neufeld*

McGill University, Department of Chemical Engineering, 3480 University St.,
Montreal, Quebec H3A 2A7, Canada

(Received 7 August 1987; revised 11 February 1988)

Microcapsules were prepared by forming a cellulose nitrate (collodion) membrane around emulsified aqueous droplets within an organic continuous phase. The control of mean diameter and size distribution of the microcapsules was achieved by varying the conditions of emulsification. Distribution data were shown to fit the log-normal distribution function. A lattice impeller permitted a greater variation of particle distribution parameters (35 to 225 μm mean diameter for a decreasing range of rev min^{-1} from 600 to 150) than was possible with a turbine impeller (72 to 91 μm for a similar range of rotational speed). Increasing emulsification time lowers the microcapsule mean diameter (from 130 to 70 μm for 1 to 3 min, respectively) and the geometric standard deviation (from 2.0 to 1.5 for 3 to 9 min, respectively). The addition of a surfactant (1% to 4% v/v) promotes the formation of smaller droplets (mean diameter from 85 to 70 μm) and leads to unimodally distributed microcapsules even at low rotational speed and duration. Finally, increasing phase ratio of internal emulsified aqueous to organic external (from 5% to 20% v/v) decreases the geometric standard deviation (from 1.7 to 1.5).

Keywords: Microcapsule; mean diameter; size distribution; microencapsulation

Introduction

Microencapsulation of enzymes and cells is an effective technique for immobilizing highly sensitive biologically active molecules and materials.¹⁻⁴ The presence of an ultra-thin, semi-permeable membrane surrounding the encapsulated contents permits transfer through diffusion of low molecular weight substrate materials and products, while limiting access to large molecular weight molecules such as antibodies or proteolytic enzymes or contaminating microorganisms. The reaction kinetics are then partially governed by Fickian diffusion and are thus indirectly proportional to the particle size, as illustrated by the decrease of the apparent activity of immobilized urease with increasing microcapsule diameter.⁵

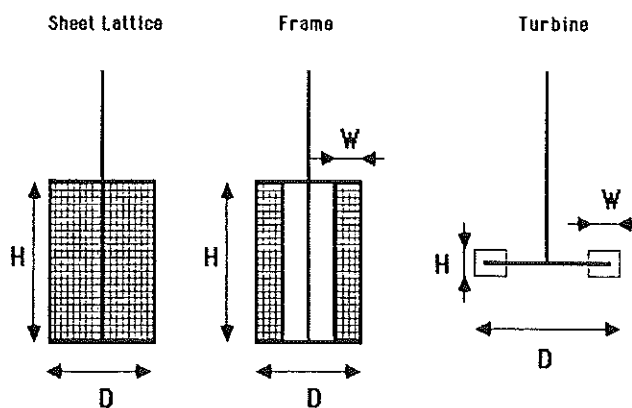
Control of the size distribution and mean diameter of microcapsules during the manufacturing process is a necessary step toward efficient reactor operation. Some consideration has been given to formulating microcapsules under the microgravity of space in an attempt to produce perfectly spherical beads of uniform membrane thickness and consistent size.⁶ Emulsification techniques for microencapsulation of enzymes have not resolved these difficulties, with resulting lack of control of diameters and size distributions and a poor understanding of the parameters affecting the physical properties of the beads.

The objective of this study was to investigate the effects of reactor and impeller geometry, rotational speed and duration, emulsifier concentration, and phase ratio on the mean diameter and size distribution of cellulose nitrate (collodion) membrane microcapsules.

* To whom all correspondence should be addressed

Table 1 Geometry and characteristic dimensions of impellers

Name	Blade number	D (mm)	H (mm)	W (mm)	Wire diameter (mm)	Mesh size (mm)
Sheet-1a	2	45	55	—	0.2	1
Sheet-1b	2	45	55	—	0.4	1
Sheet-2a	4	45	55	—	0.2	1
Sheet-2b	4	45	55	—	0.4	1
Sheet-3	4	45	55	—	0.8	2.5
Frame-1	2	45	55	10	0.2	1
Frame-2	4	45	55	10	0.2	1
Turbine	6	38	5	7	—	—



Materials and methods

Microcapsule preparation

Cellulose nitrate (collodion) microcapsules were prepared following the procedure outlined in detail by Chang,⁴ by dispersing an aqueous solution of hemoglobin in a water-saturated-ether organic phase, with the aid of an emulsifier (Span 85), to yield a water-in-oil emulsion. The only modifications introduced to this procedure concern the emulsification step, i.e., reactor and impeller geometry, rotational speed and duration, emulsifier concentration, and phase ratio. This step was followed by coacervation of a collodion membrane on the surface of the aqueous droplets. Finally, transfer of the microcapsules from the organic phase into the aqueous phase was performed by aid of a surfactant (Tween 20), and the aqueous suspension was washed several times and then sampled for size distribution determination. Normal and log-normal distribution parameters were compared.

Several authors^{7,8} describe an optimum batch size for emulsion production, when the level in the tank is equal to the tank diameter. Below this level, turbulence of the liquid surface dissipates much of the energy; above this level, the energy per unit volume decreases markedly. Mixing studies were thus conducted in a Corning 1060, 200-ml beaker, with an internal diameter of 50 mm, the total liquid (100 ml) height reaching 50 mm. Three types of impeller geometries—turbine and sheet or frame lattice impeller—were compared. Characteristic dimensions of the impellers are given in *Table 1*.

Size distribution curves and analysis

The most common particle distribution laws are the normal and the log-normal distribution functions.^{9,10}

The *normal, or Gaussian, distribution function* is expressed by:

$$\frac{d(P)}{d(d)} = \frac{100}{\sigma_a \sqrt{2\pi}} \exp\left(-\frac{(d - d_a)^2}{2\sigma_a^2}\right) \quad (1)$$

where P is the percentage of microcapsules having a diameter smaller than d , and d_a is the arithmetic mean diameter defined by:

$$d_a = \frac{\sum_n d}{n} \quad (2)$$

where n represents the number of counted microcapsules. σ_a is the arithmetic standard deviation defined by:

$$\sigma_a^2 = \frac{\sum_n (d - d_a)^2}{n} \quad (3)$$

The *log-normal distribution equation* is expressed by:

$$\frac{d(P)}{d(\log d)} = \frac{100}{\sqrt{2\pi} \log \sigma_g} \exp\left(-\frac{(\log d - \log d_g)^2}{2(\log \sigma_g)^2}\right) \quad (4)$$

where d_g is the geometric mean diameter defined by:

$$\log d_g = \frac{\sum_n \log d}{n} \quad (5)$$

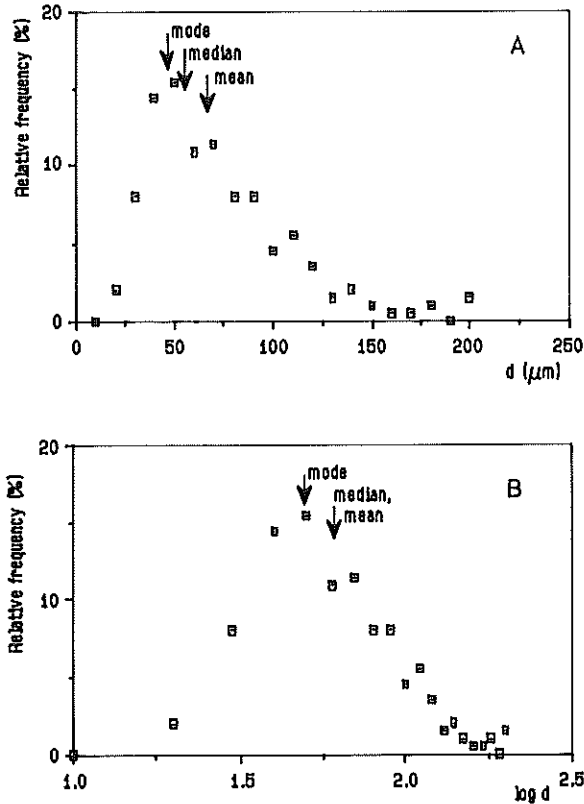


Figure 1 Collodion microcapsules distribution curves (A) Normal distribution curve; (B) log-normal distribution curve. (Sheet-1a, $N = 300 \text{ rev min}^{-1}$, $t = 3 \text{ min}$, [emulsifier] = 1% v/v, phase ratio = 10% v/v)

σ_g is the geometric standard deviation defined by:

$$(\log \sigma_g)^2 = \frac{\sum_n (\log d - \log d_g)^2}{n} \quad (6)$$

Other parameters characterizing the size distribution are the mode and median diameters. The mode diameter passes through the peak of the distribution curve, where the frequency density is maximum. The vertical line at the median divides the area under the curve into equal parts, the median diameter corresponding to a cumulative frequency of 50%. The vertical line at the mean passes through the center of gravity of a sheet of uniform thickness and density cut to the shape of the distribution curve. The mode, median, and mean coincide for symmetrical distribution.

Integration of equation (4) leads to a relation between the cumulative frequency, P , and the particle diameter, d , expressed by:

$$P = \frac{100}{\sqrt{2\pi}(\log \sigma_g)} \int_0^d \exp\left(-\frac{(\log d - \log d_g)^2}{2(\log \sigma_g)^2}\right) d(\log d) \quad (7)$$

The cumulative frequency, P , will plot a straight line of P versus the particle logarithmic diameter, $\log d$, on a normal probability graph paper, or versus

particle diameter, d , on a log-normal probability graph paper. Particle size log-normal distribution is then characterized by two parameters, the geometric mean particle diameter, d_g , identified with the median (50%) particle size of the distribution curve, and the geometric standard deviation, σ_g , obtained from the diameter value at 16% and 84% cumulative frequency.

Results

Microcapsule size distribution

Distribution curves were microscopically determined by first measuring the diameter of 200 collodion microcapsules by use of a graduated ocular. Size distribution curves obtained by plotting relative frequencies versus particle diameter, d , typically resulted in a continuous asymmetrical curve which tends toward the high diameters (Figure 1A). The normal distribution function is symmetrical about the arithmetic mean, d_a , as shown by the squared argument involving d in the exponent of equation (1). Application of the normal distribution function to asymmetrical distribution does not accurately represent all data, and can lead to erroneous conclusions for distribution parameters. However, replacing particle diameter, d , by its logarithm, $\log d$, leads to nearly symmetrical curves (Figure 1B), suggesting the application of the more representative log-normal distribution function [equation (4)]. Representation on a log-normal probability graph of the distribution data from Figures 1A and 1B is presented in Figure 2.

In the case of emulsified droplets, the size distribution is more often characterized by a right-side bias¹⁰; the log-normal distribution function is least likely to apply at the diameter extremes and most likely to fit in the midrange (80% to 90% of the diameter range). Mode, median, and mean diameters determined on the whole sample diameter range indicate a certain discrepancy (Table 2). Recalculated values of median and mean diameters without taking into account the higher diameter side bias are lower and in better accordance with the mode value.

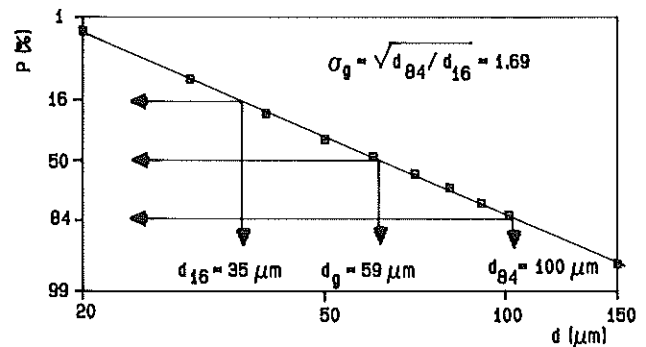


Figure 2 Collodion microcapsules size distribution on log-normal probability graph (Sheet-1a, $N = 300 \text{ rev min}^{-1}$, $t = 3 \text{ min}$, [emulsifier] = 1% v/v, phase ratio = 10% v/v)

Table 2 Distribution parameters of collodion microcapsules

Parameter	Determination method		A	B	C	
Mean diameter	Normal distribution (equation 2)	d_a	72	67	63	μm
	Log-normal distribution (equation 5)	d_g	64	61	58	μm
Standard deviation	Normal distribution (equation 3)	σ_a	36			μm
	Log-normal distribution (equation 6)	σ_g	1.6			(-)
Median	Diameter corresponding to 50% cumulative frequency		59	57	55	μm
Mode	Diameter corresponding to the maximum frequency		50			μm

A: Calculated on the entire range of particle diameters ($d_{\text{max}} = 200 \mu\text{m}$)

B: Calculated on 95% of the particle diameter range ($d_{\text{max}} = 140 \mu\text{m}$)

C: Calculated on 90% of the particle diameter range ($d_{\text{max}} = 120 \mu\text{m}$)

Sheet-1a, $N = 300 \text{ rev min}^{-1}$, $t = 3 \text{ min}$, [emulsifier] = 1% v/v, phase ratio = 10% v/v

In cases of broad distribution or wide diameter range, distribution curves obtained by measuring 200 particle diameters were discontinuous (Figure 3) and distribution parameters were difficult to determine precisely. Increasing sample size leads to a natural smoothing of the distribution curve (Figure 3) and to an evolution of the log-normal distribution parameters, geometric mean diameter, d_g , and standard deviation, σ_g , as a function of sample size. Figure 4 illustrates that typically measurement of 400 collodion microcapsules is sufficient to justify the continuum approach. Beyond this sample size, the distribution parameters remain relatively constant. The values of mean diameter obtained from replicate experiments varied less than 5%. When replicate sets of experiments were run with all but one parameter held constant, the size distribution parameters varied in a similar fashion, and the same conclusions were drawn about the influence of the varying parameters.

Impeller type and rotational speed

Collodion microcapsules prepared by using a turbine impeller result in a narrow size distribution followed by a very low tail which extends less and less as the rotational speed increases from 150 to 600 rev min^{-1}

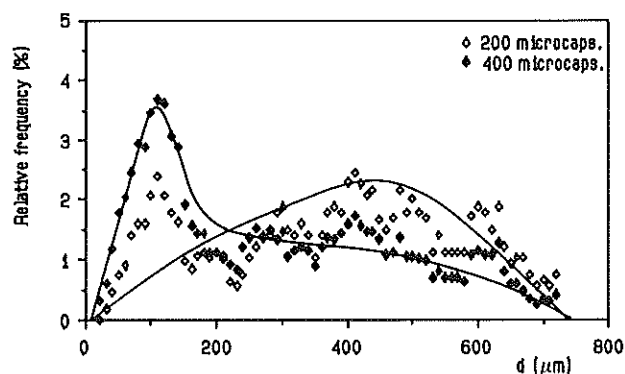


Figure 3 Size distribution of collodion microcapsules with different sample sizes (Sheet-1a, $N = 150 \text{ rev min}^{-1}$, $t = 1 \text{ min}$, [emulsifier] = 1% v/v, phase ratio = 10% v/v)

(Figure 5). In contrast, a lattice impeller under the same operating conditions yields microcapsules covering a smaller diameter range with a size distribution curve that gradually evolves from a low broad curve at 150 rev min^{-1} to a high sharp peak at 600 rev min^{-1} (Figure 6).

The corresponding size distribution parameters of collodion microcapsules prepared with the turbine impeller and with the lattice impeller are tabulated respectively in Tables 3 and 4. While the effect of an increase of turbine rotational speed is limited to the lowering of both arithmetic, σ_a , and geometric, σ_g , standard deviation, the lattice impeller rotational speed strongly affects every distribution parameter. Figure 7 presents the microcapsule geometric mean diameter, d_g , and standard deviation, σ_g , as a function of the lattice impeller rotational speed.

The log-normal distribution parameters of microcapsules prepared with different patterns of lattice impeller are tabulated in Table 5.

Emulsification time

Figure 8 presents size distribution curves for collodion microcapsules prepared by use of a lattice impeller at

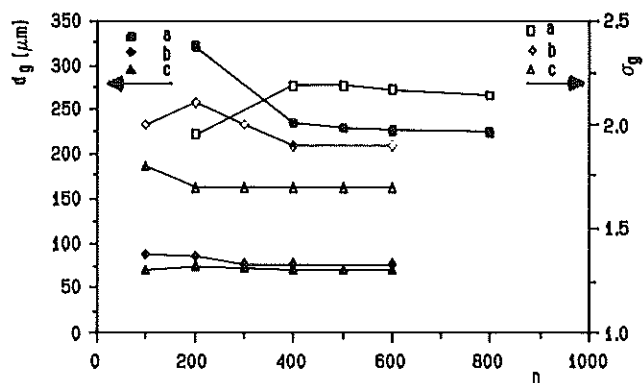


Figure 4 Influence of sample size, n , on collodion microcapsules distribution parameters [emulsifier] = 1% v/v, phase ratio = 10% v/v, a: turbine, $N = 150 \text{ rev min}^{-1}$, $t = 1 \text{ min}$; b: Sheet-1a, $N = 300 \text{ rev min}^{-1}$, $t = 1 \text{ min}$; c: Sheet-1a, $N = 300 \text{ rev min}^{-1}$, $t = 9 \text{ min}$

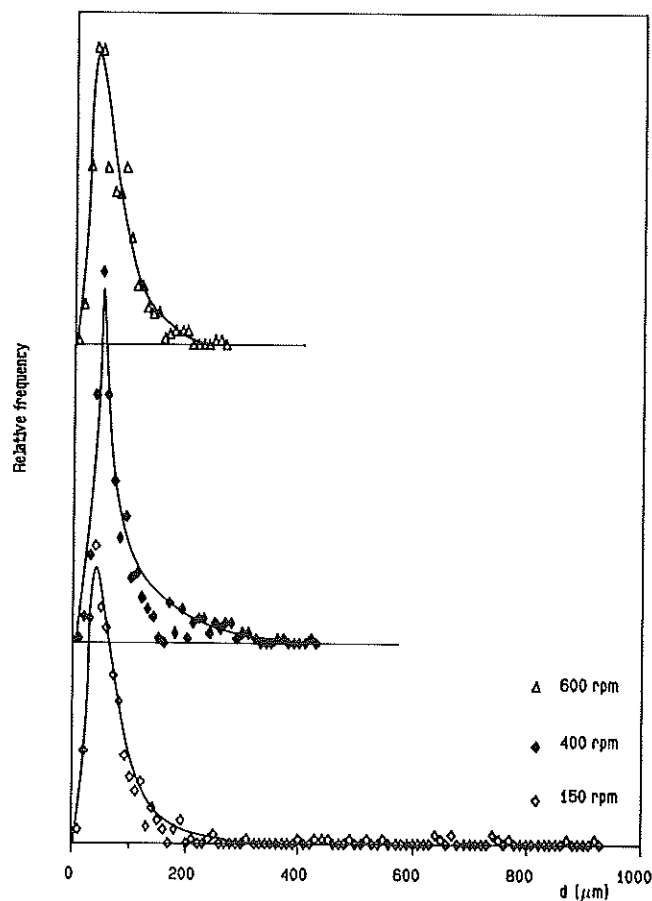


Figure 5 Influence of rotational speed, N , on size distribution of collodion microcapsules (turbine, $t = 1$ min, [emulsifier] = 1% v/v, phase ratio = 10% v/v)

different mixing time, t . Increasing mixing time results in a gradual evolution of the size distribution from a low broad curve obtained for 0.5 min of emulsification time, to a narrower distribution for 3 min of emulsification time, with a marked shift of the mode. This effect is similar to the influence of increases in rotational speed. However, any additional increase of mixing time beyond 3 min has no further effect on the distribution curve.

Table 3 Influence of turbine rotational speed, N , on the distribution parameters

Parameter	Turbine rotational speed (rev min ⁻¹)		
	150	400	600
d_a (μm)	91	89	72
σ_a (μm)	124	68	39
d_g (μm)	63	72	63
σ_g (-)	2.1	1.8	1.7
Median (μm)	54	59	57
Mode (μm)	40	50	40

$t = 1$ min, [emulsifier] = 1% v/v, phase ratio = 10% v/v

Table 4 Influence of the sheet-1a rotational speed on distribution parameters

Parameter	Sheet-1a rotational speed (rev min ⁻¹)		
	150	400	600
d_a (μm)	132	64	38
σ_a (μm)	114	25	14
d_g (μm)	98	59	35
σ_g (-)	2.1	1.5	1.5
Median (μm)	80	53	30
Mode (μm)	60	50	30

$t = 1$ min, [emulsifier] = 1% v/v, phase ratio = 10% v/v

Figure 9 shows that the particle geometric mean diameter, d_g , decreases until a limit value is reached for 3 min of stirring, while the geometric standard deviation, σ_g , continues to decrease if the stirring time is increased.

Emulsifier concentration

Increasing emulsifier concentration results in the evolution from a polymodal-type distribution curve at

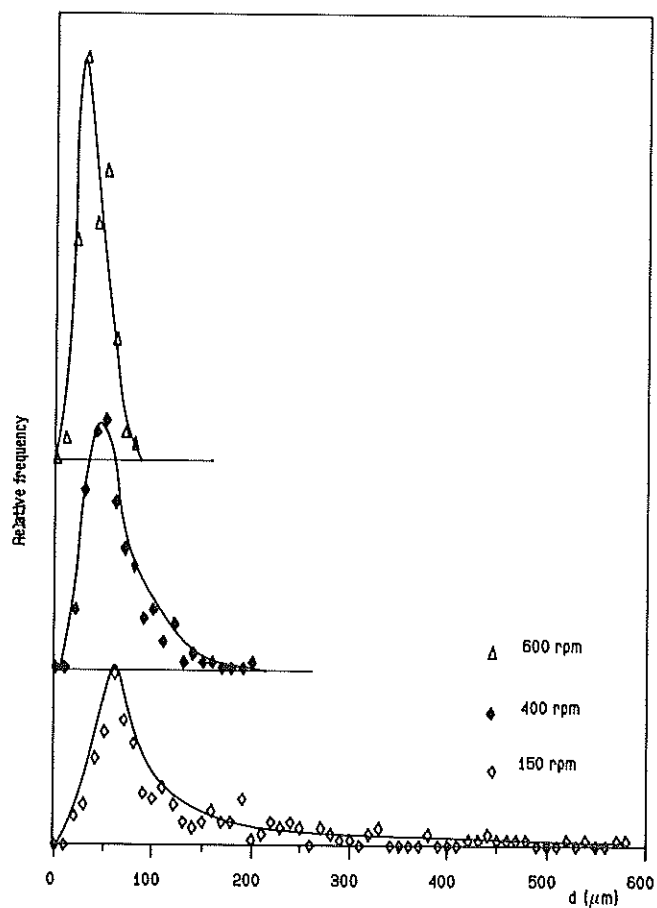


Figure 6 Influence of rotational speed, N , on size distribution of collodion microcapsules (Sheet-1a, $t = 1$ min, [emulsifier] = 1% v/v, phase ratio = 10% v/v)

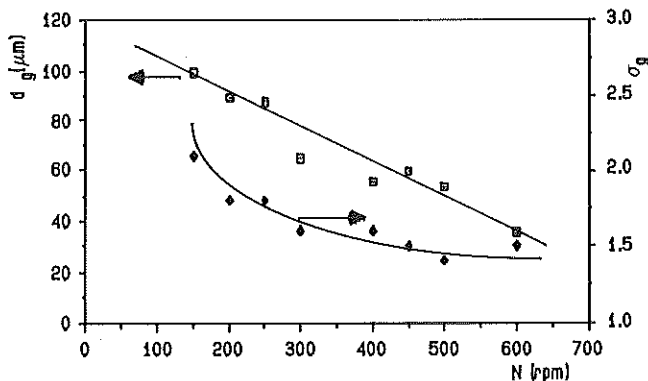


Figure 7 Evolution with rotational speed, N , of geometric mean diameter, d_g , and standard deviation, σ_g (Sheet-1a, $t = 1$ min, [emulsifier] = 1% v/v, phase ratio = 10% v/v)

low concentration of emulsifier (1% v/v) to a monomodal distribution curve at a 4% v/v concentration of emulsifier (Figure 10). Figure 11 shows that the geometric mean diameter, d_g , and standard deviation, σ_g , change in the same way as a function of the emulsifier concentration, characterized by a sharp decline at low increasing concentration, followed by an asymptotic value reached at about 4% v/v concentration of emulsifier.

Phase ratio

As the hemoglobin aqueous internal phase volume is increased with regard to the ether organic external phase volume (from 5% v/v to 20% v/v), the size distribution curve becomes more symmetrical about the mode diameter, which value increases with increase of the phase ratio (Figure 12). An increase of both arithmetic, d_a , and geometric, d_g , particle mean diameter together with a decrease of the related standard deviation, σ_a and σ_g (Table 6) also resulted from increasing the internal phase ratio.

Discussion

The size distribution of collodion microcapsules prepared following the procedure proposed by Chang⁴

Table 5 Influence of the lattice impeller design on distribution parameters

Impeller design	A		B	
	d_g (μm)	σ_g (-)	d_g (μm)	σ_g (-)
Sheet-1a	95	1.7	142	2.0
Sheet-1b	-	-	115	1.9
Sheet-2a	99	1.7	113	2.2
Sheet-2b	-	-	109	1.9
Sheet-3	-	-	99	2.1
Frame-1	90	1.7	-	-
Frame-2	96	1.7	-	-

[emulsifier] = 1% v/v, phase ratio = 10% v/v
A: $N = 300$ rev min^{-1} , $t = 6$ min, B: $N = 150$ rev min^{-1} , $t = 1$ min

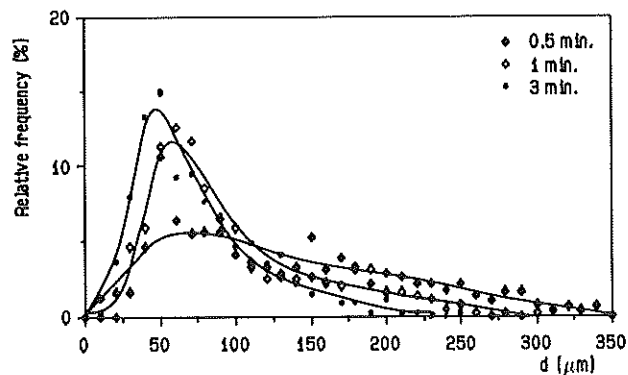


Figure 8 Influence of emulsification time, t , on size distribution of collodion microcapsules (Sheet-1a, $N = 300$ rev min^{-1} , [emulsifier] = 1% v/v, phase ratio = 10% v/v)

is primarily determined by the emulsification step. The emulsification process can be described in two stages.¹⁰⁻¹² Initially, disruption of droplets leads to the dispersion of the internal phase. The pressure to be externally applied on the droplet (determined by the Laplace pressure) is proportional to γ/d^2 , where γ is the interfacial tension and d is the drop diameter.¹⁰ This expression shows that the lowering of the droplet size requires an increasing energy input. The second stage involves coalescence of two drops into one, which diminishes the interfacial area and thus the interfacial surface energy leading to a more stable state. Any emulsion is inherently unstable and will eventually break down to form two separate phases, because the interfacial surface energy is proportional to the high interfacial surface area.¹⁰ Any change in the system that reduces the total surface area and thus energy will bring the system to a more stable state.

Examination of size distribution curves of microcapsules prepared by use of a turbine type impeller operating at different rotational speed reveals that these distributions are characterized by two zones (Figure 5): a log-normal shaped distribution located in

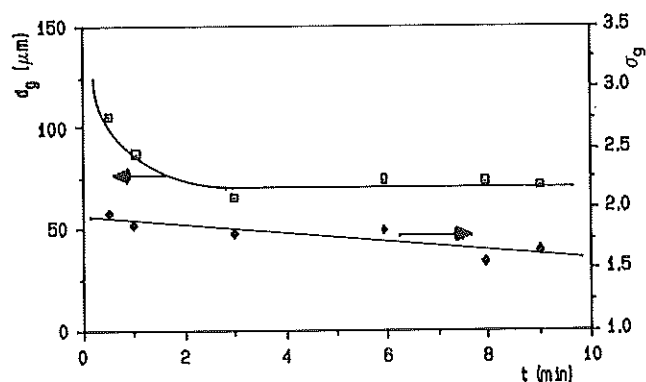


Figure 9 Evolution with emulsification time, t , of geometric mean diameter, d_g , and standard deviation, σ_g (Sheet-1a, $N = 300$ rev min^{-1} , [emulsifier] = 1% v/v, phase ratio = 10% v/v)

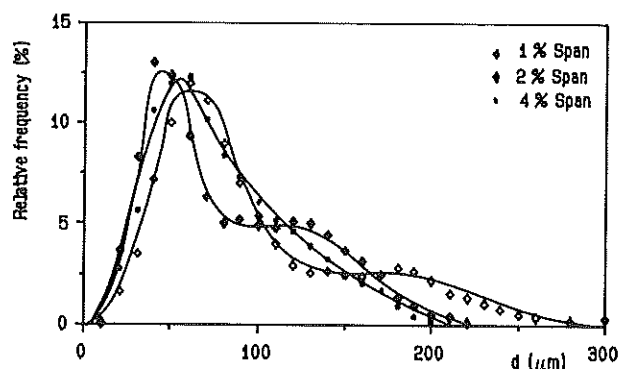


Figure 10 Evolution of size distribution with emulsifier concentration.

a: 1% v/v span, b: 2% v/v span, c: 4% v/v span
(Sheet-1a, $N = 250 \text{ rev min}^{-1}$, $t = 1 \text{ min}$, phase ratio = 10% v/v)

the small diameter range followed by a more or less extending right-side bias. Turbine stirrers are characterized by a high flow resistance. Most of the mechanical energy provided is concentrated in a small volume in the vicinity of the impeller, where the high velocities and shear stresses overcome the surface forces of the fluid to be dispersed,¹³ and where the break-up process requiring high shear forces will be predominant. When the turbine impeller is operated at low rotational speed, high shear stresses develop in the vicinity of the impeller, causing the disruption of the internal phase into small droplets (log-normal shaped distribution area). At distant locations from the impeller, as at the bottom of the tank, the available energy is not sufficient to support the transport of the dense internal phase to the impeller blades, and the coalescence process becomes more frequent, leading to the formation of larger droplets (right-side bias distribution area). An increase of turbine rotational speed results in an increase and better distribution of power input in the reactor, thereby promoting the disruption process in a larger zone around the impeller. The acceleration of disruption or the lowering of the coalescence rate,

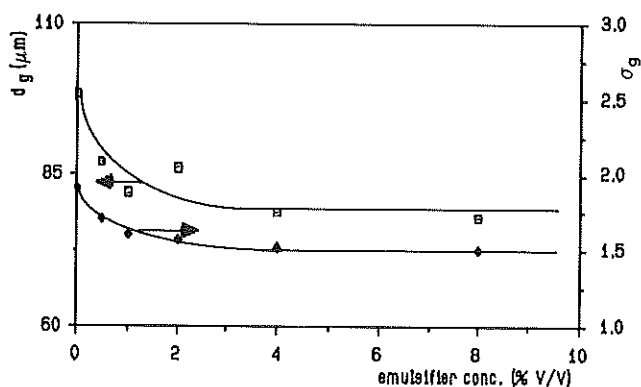


Figure 11 Evolution with emulsifier concentration of geometric mean diameter, d_g , and standard deviation, σ_g
(Sheet-1a, $N = 250 \text{ rev min}^{-1}$, $t = 1 \text{ min}$, phase ratio = 10% v/v)

Table 6 Influence of the phase ratio on distribution parameters

Parameter		Phase ratio (% v/v)		
		5	10	20
d_a	(μm)	114	126	124
σ_a	(μm)	56	59	43
d_g	(μm)	100	110	115
σ_g	(-)	1.7	1.7	1.5
Median	(μm)	100	110	120
Mode	(μm)	70	90	120

Sheet-1a, $N = 300 \text{ rev min}^{-1}$, $t = 8 \text{ min}$, [emulsifier] = 1% v/v

provided by a higher rotational speed, explains the progressive disappearance of larger microcapsules as the turbine rotational speed increases (Figure 5). The relatively constant mode and mean particle diameters (Table 3) over the entire range of turbine rotational speed are due to the small relative percentage of the larger microcapsules.

Lattice impellers are designed to mix the entire vessel contents and dispense the energy more uniformly throughout the liquid⁸; pumping and shear effects are equally distributed in the entire vessel volume. Microcapsules obtained by use of a lattice impeller (Figure 6) illustrate a good fitting of the distribution data with the log-normal distribution function over the entire range of rotational speed. These observations can be partially explained by the fact that the mechanical energy input to the system is more homogeneously distributed in the bulk of the liquid, even at low rotational speed. The thermodynamic energy necessary to increase the surface area leading to a decrease of particle size is provided by increasing the impeller speed. The maximum frequency diameter, or mode, is markedly shifted toward smaller values, and the corresponding relative frequency increases strongly as the lattice impeller speed increases. Both geometric mean diameter, d_g , and standard deviation, σ_g , decrease strongly as the rotational speed increases

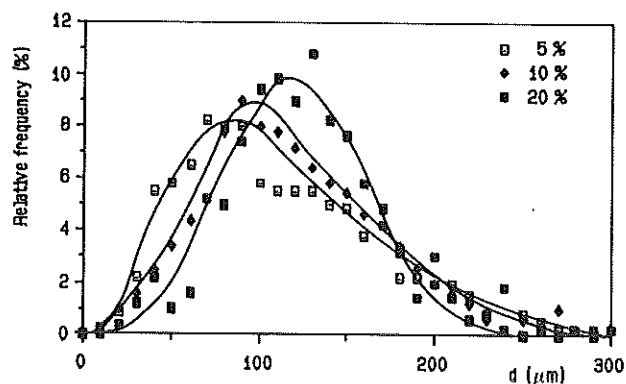


Figure 12 Influence of phase ratio on collision microcapsules size distribution.

a: 5% v/v, b: 10% v/v, c: 20% v/v
(Sheet-1a, $N = 300 \text{ rev min}^{-1}$, $t = 8 \text{ min}$, [emulsifier] = 1% v/v)

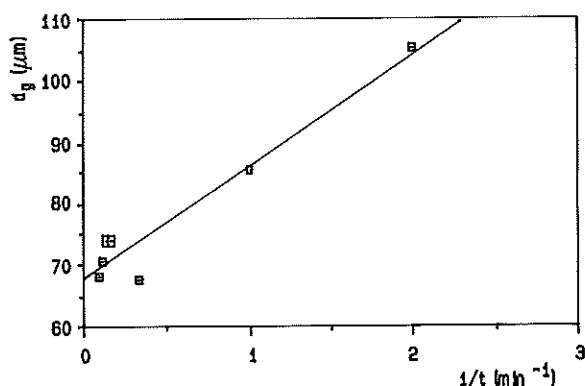


Figure 13 Evolution with emulsification time reciprocal, $1/t$, of collision microcapsule geometric mean diameter, d_g (Sheet-1a, $N = 300 \text{ rev min}^{-1}$, [emulsifier] = 1% v/v, phase ratio = 10% v/v)

(Table 4, Figure 7). Table 5 shows that the type of lattice (wire diameter, mesh dimensions, sheet or frame shape and number) has only a small effect on the microcapsule size distribution parameters, other operating conditions being maintained constant.

Both geometric mean diameter, d_g , and geometric standard deviation, σ_g , of microcapsules prepared with a turbine type impeller are relatively constant over the whole range of rotational speed. In contrast, the distribution parameters of microcapsules prepared by use of the lattice type impeller are a function of the stirrer rotational speed. A real control of the microcapsule size distribution is then only possible with lattice impeller. For these reasons, in the remainder of the study, the lattice impeller rather than the turbine type was chosen.

For a given set of operating conditions, increasing mixing time, t , corresponding to an increase of power input, results in a decrease of the geometric particle diameter, d_g . This effect diminishes with time as illustrated by the asymptotic value reached for the geometric mean particle diameter, d_g . However, increasing emulsification duration, t , beyond 3 min involves a further decrease of the geometric standard deviation, σ_g , indicating that the equilibrium state is not reached.

A more accurate measure of change in particle size as a function of the emulsification duration, t , may be obtained by plotting the geometric mean particle diameter, d_g , versus the reciprocal of stirring time, $1/t$.⁷ This results in a straight line (Figure 13). The intercept with the particle diameter axis, for $t = \infty$, is the smallest geometric mean diameter, d_g , that can be achieved under the emulsification conditions. This provides an accurate way to predict geometric mean particle diameter with emulsification time when the ultimate diameter for a particular operation is known.

A stable emulsion will be characterized by an equilibrium state between disruption and coalescence. This equilibrium state can be promoted by addition of surface active agents lowering the interfacial tension,

γ , and thus the Laplace pressure, facilitating the deformation and disruption of the drops, for a given stirring rate. At low to moderate emulsifier concentrations, the emulsifier acts primarily as a surfactant, facilitating the dispersion process, thus involving the decrease of the geometric mean particle diameter, d_g , as illustrated by the sharp decline in the beginning of the curve on Figure 11. At a higher emulsifier concentration, the effect of increase in external phase viscosity becomes more and more important, preventing the coalescence process, thus involving a decrease of the geometric standard deviation, σ_g (Figure 11), due to the disappearance of the secondary higher diameter peak (Figure 10).

Finally, particle size increases as phase ratio increases (Table 6), because of increased coalescence rate. The distribution curves (Figure 12) become more and more symmetrical about the mode, thus normally distributed, indicating a better equilibrium between disruption and coalescence.

Reduction of the microcapsule size dispersion, necessary for a good control of the biochemical process involving the encapsulated product, can be achieved by selecting optimum values for emulsification time (t equal to at least 3 min), emulsifier concentration (4% v/v), and phase ratio (20% v/v), in terms of minimal geometric standard deviation, energy cost, and product consumption. Greater control of mean diameter ranging from 35 to 225 μm is attained by use of a lattice impeller instead of turbine, secondly by selection of an appropriate rotational speed.

Acknowledgement

This work was financially supported by a strategic research grant from the National Sciences and Engineering Research Council of Canada.

Nomenclature

d	particle diameter	(μm)
d_a	arithmetic mean diameter	(μm)
d_g	geometric mean diameter	(μm)
N	impeller rotational speed	(rev min^{-1})
n	number of particles	(-)
P	cumulative frequency	(%)
t	emulsification duration	(min)
σ_a	arithmetic standard deviation	(μm)
σ_g	geometric standard deviation	(-)
γ	interfacial tension	(Ns^{-2})

References

- 1 Chang, T. M. S. *Artificial Cells* Charles C. Thomas Publisher, Springfield, IL, 1972, pp. 15-26
- 2 Trampler, J. *Trends Biotechnol.* 1985, 3(2), 45-50
- 3 Chang, T. M. S. MacIntosh, F. C. and Mason, S. G. *Can. J. Physiol. and Pharmacol.* 1966, 44, 115-128
- 4 Chang, T. M. S. in *Biomedical Applications of Immobilized Enzymes and Proteins* (Chang, T. M. S., ed.) Plenum Press, New York, 1977, Vol. 1, pp. 69-90
- 5 Dueck, C. L., Neufeld, R. J., Chang, T. M. S., *Can. J. Chem. Eng.* 1986, 64, 540-546

- 6 Birenbaum, R. *Can. Research* October 1986, 4-6
- 7 Rounsley, R. R. *A.I.Ch.E. J.* 1983, **29(4)**, 597-603
- 8 Oldshue, J. Y. *Fluid Mixing Technology* Chemical Engineering McGraw Hill Publications, New York, 1983
- 9 Terence Allen *Particle Size Measurement* Chapman and Hall Ltd., New York, 1981, pp. 103-164
- 10 Becher, P. *Encyclopedia of Emulsion Technology* Dekker, New York, 1983, *Vol. 1*, pp. 369-404
- 11 Bennet, H. Bishop, J. L., Wulfinhoff, M. F., *Practical Emulsions: Material and Equipment* Chemical Publishing Company, New York, 1968, *Vol. 1*
- 12 Dinesh O. Shah *Macro- and Microemulsions: Theory and Applications* A.Ch.S. Symposium Series, 1985, **272**
- 13 Mersmann, A. B. *et al. A Short Course on Mixing Technology* (Mujumdar, A. S., ed.) McGill University, 1982